

Effects of epitaxial lift-off on interface recombination and laser cooling in GaInP/GaAs heterostructures

Babak Imangholi,^{a)} Michael P. Hasselbeck, and Mansoor Sheik-Bahae

Department of Physics and Astronomy, University of New Mexico, Albuquerque, New Mexico 87131

Richard I. Epstein

Los Alamos National Laboratory, Los Alamos, New Mexico 87545 and Department of Physics and Astronomy, University of New Mexico, Albuquerque, New Mexico 87131

Sarah Kurtz

National Renewable Energy Laboratory, Golden, Colorado 80401

(Received 30 August 2004; accepted 28 December 2004; published online 15 February 2005)

Photoluminescence of GaAs passivated with GaInP is studied over the temperature range 7–450 K. Different photocarrier recombination mechanisms are identified as the temperature changes. An interface recombination velocity of less than 0.6 cm/s is measured at 300 K. Lift-off processing inhibits but does not preclude laser cooling of GaAs. © 2005 American Institute of Physics. [DOI: 10.1063/1.1868068]

Long recombination lifetimes in semiconductors are essential for realization of efficient solar cells. Recombination pathways include bulk and surface defect trapping, photon emission at the band gap, and Auger scattering.¹ Our measurements of recombination in GaAs are motivated by laser cooling (i.e., optical refrigeration), in which heat is removed from the semiconductor by anti-Stokes luminescence.^{2,3} If optical excitations near the band gap energy decay with high efficiency in the form of blueshifted radiation, net cooling can occur.

For low density optical excitation of bulk GaAs devices, the surface recombination velocity drives the nonradiative recombination rate. Passivation schemes to mitigate deleterious surface recombination have been implemented using layered heterostructures grown by MBE or MOCVD.^{1,4,5} A layer of bulk GaAs is sandwiched between thin layers (<1 μm) of semiconducting alloys with higher band gap energy (Fig. 1 inset). Lattice-matched AlGaAs, AlInP, and GaInP have been used for passivation as well as degenerate layers of GaAs. Band energy discontinuities prevent mobile carriers in GaAs from migrating through the passivating material to the surface; spatial separation of electrons and holes at the interface also inhibits recombination.

To process a device such as a solar cell or optical refrigerator, one separates the grown heterostructure from the substrate, which can be semi-insulating GaAs. Heterostructure lift-off is accomplished by growing an AlAs release layer between the device and substrate; this layer is removed using a hydrofluoric acid etch.² We show that lift-off processing can affect interface recombination.

Olson *et al.* performed a temperature-dependent study of recombination with GaAs heterostructures.¹ They found that GaInP passivation provides the longest nonradiative lifetimes and attributed this to the absence of oxygen-related defects at the interface. This work placed an upper limit on the interface recombination velocity ($S < 1.5$ cm/s) based on photoluminescence measurements at room temperature with the heterostructure attached to the substrate. In this letter, we

report measurements of photoluminescence in GaInP/GaAs before and after lift-off over a wide temperature range (7–450 K), which allows the different recombination mechanisms to be clearly separated.

We characterize the carrier lifetime using time-resolved photoluminescence. The time rate of change of the optically excited electron-hole pair density (N) is

$$\frac{dN}{dt} = G - AN - \eta_e B N(N + N_x) - \eta_e B_x N N_x^0 - CN^3, \quad (1)$$

where G is the excitation rate, A accounts for nonradiative recombination via bulk and surface defects, B is the band gap radiative recombination coefficient of GaAs, B_x is the coefficient for recombination to the impurity level, C describes the three-body Auger scattering process, N_x and N_x^0 are the densities of ionized and unionized impurities, respectively, and η_e is the luminescence extraction efficiency that accounts for photon recycling caused by bulk absorption and surface reflections.⁴ These parameters are all temperature-dependent. We ignore diffusion because it does not influence the measured lifetime for our geometry.⁶ Bulk defect recombination (i.e., the Shockley-Read-Hall process) is small compared to interface recombination in high-quality samples such as ours.⁴ The nonradiative recombination rate due to the interface is $A = 2S/d$, where S is the recombination velocity and d is the thickness of the bulk layer. The defect sites that cause interface recombination are thermally activated at higher temperature;⁷ the temperature dependence of the recombination velocity is $S(T) = S_0 \exp(-E_a/kT)$ where E_a is the activation energy of the defect state. The luminescence signal is proportional to the radiative terms in Eq. (1) and gives a direct measure of the nonequilibrium carrier concentration.

The heterostructures used in our experiments (shown schematically in the upper left inset of Fig. 1) are grown by atmospheric-pressure chemical vapor deposition using trimethylgallium, trimethylindium, arsine, phosphine, trimethylaluminum, and disilane in a hydrogen carrier gas using GaAs substrates.¹ The nominally undoped GaAs active layers are clad with Si-doped GaInP. Standard photolithography

^{a)}Electronic mail: babak@unm.edu

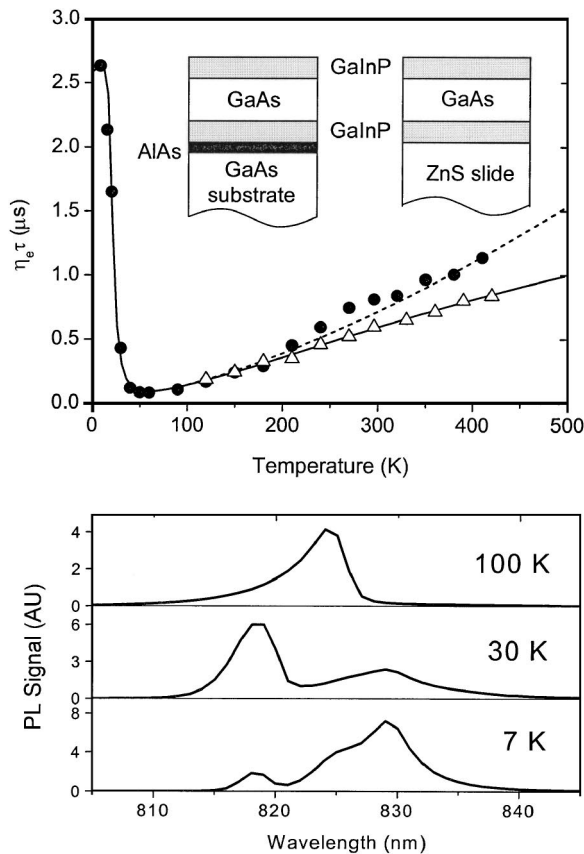


FIG. 1. Top: Photoluminescence lifetime of GaInP/GaAs ($d=1.0 \mu\text{m}$) heterostructures before lift-off (closed circles) and after lift-off and bonding to a ZnS slide (triangles). The dotted curve is from a model that ignores interface recombination; solid curve includes interface recombination. Inset top-left: Schematic of unprocessed sample; Inset top-right: After lift-off and bonding to ZnS. Bottom: Time-integrated photoluminescence of the unprocessed sample revealing acceptor freeze-out at $T \leq 30 \text{ K}$.

and plasma vertical etching produce individual samples in the form of 1-mm-diam disks. Two different GaAs thicknesses ($d=0.5$ and $1 \mu\text{m}$) are studied. In one set of experiments, the heterostructure is kept attached to the GaAs substrate. We compare the photoluminescence to that of devices which are released from the substrate by etching the AlAs layer shown in Fig. 1. After lift-off, the sample is bonded to a ZnS slide, as in a laser cooling device (upper right inset of Fig. 1).^{3,8}

A pulsed diode laser ($\lambda=670 \text{ nm}$, pulse duration: 5 ns , energy: 30 pJ) uniformly illuminates the sample (beam area: $\sim 1 \text{ cm}^2$) at a repetition rate of 20 kHz . The semiconductor heterostructure is attached to the coldfinger of a closed-cycle helium optical cryostat (Janis Research). A multi-alkali photomultiplier tube detects time-resolved, spectrally integrated luminescence via photon counting.⁹ We analyze the late-time tail of the photoluminescence signal so the influence of nonlinear bimolecular (BN^2) and Auger (CN^3) recombination of photocarriers in Eq. (1) is minimized. A single exponential fits these data indicating the nonlinear processes are insignificant.

Data showing the temperature-dependence of photoluminescence lifetime before and after lift-off for the $d=1 \mu\text{m}$ heterostructure are presented in Fig. 1 (top). The late-time photoluminescence is scaled by the theoretical extraction efficiency (η_e) to account for different amounts of photon recycling that occur in the two device geometries.^{3,10} At tem-

perature $T > 250 \text{ K}$, a decreased lifetime for the processed sample (triangles) indicates an increase of the nonradiative recombination rate. We believe this is caused by defects introduced by flexing of the nonrigid heterostructure upon release from the substrate. In the range $100 \text{ K} < T < 300 \text{ K}$, radiative recombination from the conduction to valence band governs the decay signal for both samples. Radiative recombination scales with temperature as $B=B_0(T/300\text{K})^{-3/2}$. The pronounced rise that occurs below 40 K for the unetched sample reflects the onset of impurity (i.e., acceptor) freeze-out in GaAs. The increase of photoluminescence lifetime is due to the disappearance of extrinsic holes in the valence band, which inhibits conduction- to valence-band recombination.⁵ We have no low temperature data for the sample bonded to the ZnS slide because the slide insulates the coldfinger from the sample, preventing it from reaching temperatures below 90 K .

We confirm the presence of impurity level recombination with time-integrated, spectrally resolved photoluminescence data shown in Fig. 1 (bottom). For temperatures $T \leq 30 \text{ K}$, the luminescence is dominated by conduction-to-acceptor recombination at $\lambda \approx 829 \text{ nm}$, which is distinguishable from the band gap wavelength of 818 nm . At higher temperature, the acceptor peak disappears due to the increased electron population in this state. Only direct band gap recombination ($\lambda \approx 824 \text{ nm}$) is visible at 100 K ; the redshift is due to the temperature variation of the band gap energy. The impurity peak corresponds to an activation energy of $\sim 35 \text{ meV}$, which is typical for acceptors; donor activation energies are an order of magnitude smaller. The acceptors are likely carbon and/or zinc residue in the MOCVD chamber.

The data are analyzed with a self-consistent model using Eq. (1) and the condition of space-charge neutrality. An acceptor concentration $N_x=3.5 \times 10^{15} \text{ cm}^{-3}$ is derived from measured lifetimes in the range $60 < T < 300 \text{ K}$; the recombination velocity (S_0) and interface defect activation energy (E_a) are obtained at high temperature. We model conduction-acceptor radiative recombination as described in Ref. 11 and deduce $B_x=1.3 \pm 0.1 \times 10^{-10} \text{ cm}^3 \text{ s}^{-1}$ at 7 K .

A model that ignores interface recombination (dotted curve in Fig. 1) describes the behavior of the unetched sample. It cannot, however, account for the reduced lifetime of the sample after lift-off and bonding. Including interface recombination (solid curve in Fig. 1) allows us to fit the data for the bonded sample with $E_a=18 \text{ meV}$ and $S_0=3.1 \pm 0.6 \text{ cm/s}$, where we assume lift-off introduces an insignificant number of bulk defects. This corresponds to a nonradiative lifetime of $27 \mu\text{s}$ at room temperature. Even though interface recombination is evident in the data for this sample, the high temperature lifetime is primarily driven by radiative recombination.

For the $d=1 \mu\text{m}$ heterostructure, we estimate an upper limit for the interface recombination velocity before lift-off processing of $S < 0.6 \text{ cm/s}$ at 300 K corresponding to a lifetime $d/2S > 82 \mu\text{s}$. The $d=0.5 \mu\text{m}$ sample exhibits qualitatively similar behavior but is found to have an interface recombination lifetime that is $\sim 2 \times$ smaller. This confirms the $1/d$ scaling of the surface recombination rate and shows that the interface recombination velocity is approximately the same in both samples.

As the temperature decreases below 300 K , interface recombination becomes even less efficient and radiative recombination predominates. This is a condition highly favor-

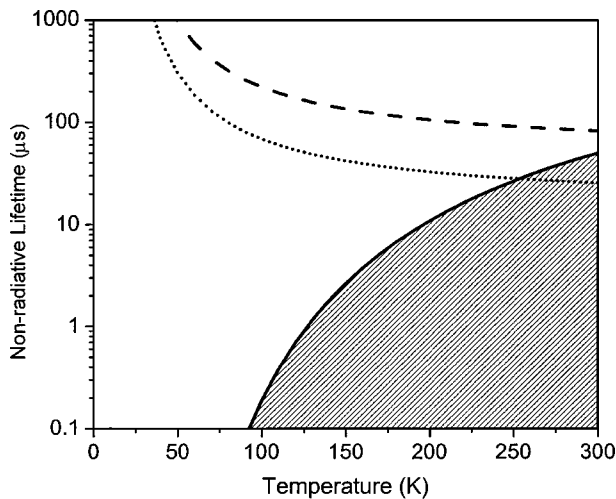


FIG. 2. Analysis of laser cooling for a $1.0 \mu\text{m}$ GaAs layer as a function of temperature. The solid curve is the calculated minimum nonradiative lifetime ($1/A$) to achieve net cooling using Eq. (2) with $\tau_0=500 \text{ ns}$ and $\eta_e=10\%$. The shaded (unshaded) region corresponds to net heating (cooling). Dashed curve is the measured surface recombination lifetime of the unprocessed sample; dotted line is obtained after lift-off.

able for attaining laser cooling. The nonradiative recombination rate at which heating just balances laser cooling defines a “break-even” lifetime ($1/A$). To attain cooling the system must be designed such that³

$$\frac{\eta_e^2}{A} \geq \tau_0 \left[\frac{T}{300 \text{ K}} \right] \exp \left[\beta \left(1 - \frac{300 \text{ K}}{T} \right) \right], \quad (2)$$

which is derived from the known temperature scaling of radiative and Auger recombination. The coefficient β is obtained by fitting temperature-dependent Auger data; for GaAs $\beta=2.24$.¹² We define a characteristic lifetime:

$$\tau_0 = \frac{4C_0}{B_0^2} \left(\frac{E_g}{0.026} \right)^2, \quad (3)$$

where B_0 , C_0 , and E_g are the radiative and Auger coefficients and band gap energy (eV), respectively, at 300 K. For GaAs, the value of τ_0 is in the range $100 \text{ ns} < \tau_0 < 2 \mu\text{s}$ due to uncertainty in B_0 and C_0 .¹³ The calculated break-even lifetime for a $d=1 \mu\text{m}$ device bonded to a ZnS dome is shown by the solid curve in Fig. 2 as a function of semiconductor temperature. The ZnS dome serves as a spherical lens to remove luminescence from the heterostructure.² Nonradiative lifetimes above the solid curve are conducive to net cooling; heating occurs below the curve (shaded region). The

measured recombination velocity parameters and temperature scaling of S allow us to calculate the nonradiative lifetimes for both unetched (dashed curve) and processed (dotted curve) samples. We find that even with the lifetime degradation that occurs with lift-off, conditions for net cooling of a GaInP/GaAs heterostructure are favorable at temperatures $T < 250 \text{ K}$.

The nonradiative interface recombination rate (A) and luminescence removal efficiency (η_e) both depend on the thickness of the GaAs layer (d). The optimum condition for laser cooling occurs when the quantity η_e^2/A is maximum.³ This defines an ideal GaAs thickness of $0.5 < d < 1.0 \mu\text{m}$ for a passivated heterostructure bonded to a ZnS dome.

In summary, although lift-off processing increases the interface recombination velocity, our studies show that net laser cooling of a GaAs/GaInP heterostructure should be possible when the temperature is below 250 K.

The authors acknowledge helpful contributions from D. Bender, B. Fuchs, K. Malloy, and D. Seletskiy. This work is supported by the National Aeronautics and Space Administration (Grant No. NAG5-10373) and the Air Force Office of Scientific Research through Grant Nos. F49620-0201-0057, F49620-0201-0059, and Multi-Disciplinary University Research Initiative FA9550-04-1-0356. This work was carried out in part under the auspices of the U.S. Department of Energy.

¹J. M. Olson, R. K. Ahrenkiel, D. J. Dunlavy, B. Keyes, and A. E. Kibbler, *Appl. Phys. Lett.* **55**, 1208 (1989).

²H. Gauck, T. H. Gfroerer, M. J. Renn, E. A. Cornell, and K. A. Bertness, *Appl. Phys. A: Mater. Sci. Process.* **64**, 143 (1997).

³M. Sheik-Bahae and R. I. Epstein, *Phys. Rev. Lett.* **92**, 247403 (2004).

⁴R. K. Ahrenkiel, D. J. Dunlavy, B. Keyes, S. M. Vernon, T. M. Dixon, S. P. Tobin, K. L. Miller, and R. E. Hayes, *Appl. Phys. Lett.* **55**, 1088 (1989).

⁵L. M. Smith, D. J. Wolford, R. Venkatasubramanian, and S. K. Ghandi, *Appl. Phys. Lett.* **57**, 1752 (1990).

⁶G. W. t'Hooft and G. van Opdorp, *J. Appl. Phys.* **60**, 1065 (1986).

⁷C. H. Henry and D. V. Lang, *Phys. Rev. B* **15**, 989 (1977).

⁸B. Imangholi, M. P. Hasselbeck, and M. Sheik-Bahae, *Opt. Commun.* **227**, 3337 (2003).

⁹Low signal levels prevent the luminescence from being both temporally and spectrally resolved.

¹⁰The extraction efficiency (η_e) for each device is calculated numerically using software from ZEMAX Development Corp., San Diego, CA 92117.

¹¹P. K. Basu, *Theory of Optical Processes in Semiconductors* (Clarendon, Oxford, 1997), p. 220.

¹²M. Takeshima, *J. Appl. Phys.* **58**, 3846 (1985).

¹³J. Piprek, *Semiconductor Optoelectronic Devices* (Academic/Elsevier, Burlington, 2003).